New Process for the Treatment of Polluted Water Using the Coupling of Nanoparticles and Magnetic

Hajer Tlili , Anis Elaoud * , Nedra Asses , Karima Horchani-Naifer , Mounir Ferhi

Posted Date: 12 October 2023

doi: 10.20944/preprints202309.1243.v2

Keywords: water treatment; nanoparticles; Fe3O4; magnetic field

Article

New Process for the Treatment of Pollutants in Waste Water Using Coupling of Nanoparticles and Magnetic

Hajer Tlili [1,2], Anis Elaoud [2,3,*], Nedra Asses [2], Karima Horchani-Naifer [1], Mounir Ferhi [1], Gerardo F. Goya [4,5] and Jesús Antonio Fuentes-García [4,5]

[1] Physical Chemistry Laboratory for Mineral Materials and their Applications, National Center for Research in Materials Sciences CNRSM, Technopole Borj Cedria, Tunisia
[2] Higher Institute of Environmental Sciences and Technologies - Carthage University, Tunisia
[3] Laboratory of Probability and Statistics, Faculty of Sciences Sfax, University of Sfax, Tunisia
[4] Departamento de Física de la Materia Condensada, Facultad de Ciencias, Universidad de Zaragoza, 50009 Zaragoza, Spain
[5] Instituto de Nanociencia y Materiales de Aragón (INMA), CSIC-Universidad de Zaragoza, 50018 Zaragoza, Spain
* Correspondence: anis.aoud@yahoo.fr

Abstract: Many of the current strategies for removing pollutants from water are based on nanomaterials and nanotechnology. Lower values of Biological Oxygen Demand (BOD5) and Chemical Oxygen Demand (COD) in water results in reduction in the amount of oxidizable pollutants. We present a study on the reduction of COD and BOD5 in water from Wadi El Bey River (Tunisia), using magnetite nanoparticles (MNPs) and magnetic fields. The COD and BOD5 removal attained values higher than 50% after 60 min, with optimum efficiency at pH values of ≈8 and for MNPs concentrations of 1 g/L. The use of a dc magnetic fields showed an increase of COD and BOD5 removal from 61% to 76% and 63% to 78%, respectively. This enhancement is discussed in terms of the MNPs coagulation induced by the magnetic fields and the adsorption of ionic species onto the MNPs surface due to Fe_3O_4 affinity.

Keywords: magnetite; Biological Oxygen Demand (BOD_5); Chemical Oxygen Demand (COD); magnetic field

1. Introduction

The availability of drinking water has become one of the most pressing environmental concerns nowadays. Human activities generate wastes that can affect the running water, modifying its chemical, physical, biological characteristics, and the possibility to be consumed. The water quality is an important factor to determine if the water could affect human health and ecosystem´s balance [1]. Hence, the development of new routes and technologies to eliminate pollutants is needed in order to recover the water quality and the possibility of contribute with the water cycle.

Water quality assessment and sanitation infrastructure have not matched population growth and industrial development, especially in underdeveloped countries[2]. Rivers continue to be the main source of water for domestic, industrial and agricultural activities, and wastewater is often discharged directly into basins without any treatment, causing severe degradation of water quality and the receiving environment. Therefore, awareness of surface water quality importance to public health and environment has increased, and many studies have been devoted to assessing surface water quality and preventing its impact on the environment [3].

Tunisia faces water shortages with only about 450 m^3/inhabitant/year of available fresh water due to its arid to semi-arid climate [4].There is an urgent need to protect water resources, address water scarcity and meet some of the increased demand. The Wadi El Bey watershed (475 km^2) is located in

 doi:10.20944/preprints202309.1243.v2

the northeast of Tunisia and flows through the Grombalia, Beni Khaled and Soliman plains [5]. It is located between Jebal Bouchoucha and Jebal Halloufa to the west, Jebal Abderrahman to the east, Jebal Reba El Ain to the south and the Gulf of Tunis to the north [6]. The Wadi El Bey River receives "pre-treated" water from different local industrial manufactures, however, still affecting negatively the physicochemical and microbiological quality of the river flow water.

For the water quality determination, the biochemical oxygen demand (BOD_5) and the chemical oxygen demand (COD) are the most used parameters to evaluate the quality of water and their standard values depends on the water usage. The BOD_5 refers to the mass of dissolved oxygen (DO) consumed by living microorganisms as they break down organic matter in water, while the COD is the amount of oxygen consumed when water is chemically oxidized [7].

A high level of physicochemical parameters such as BOD_5 and COD causes the reduction of dissolved oxygen in water and low concentrations affects eutrophication and harm aquatic life. Therefore, it is important to reduce the COD and BOD_5 parameters to values that allow sewage to be discharged into the river on a secure way. COD values less than 30 mg/L and BOD_5 values less than 250 mg/L according with the ISO standard (International Organization for Standardization) requirements for the discharge of polluted water to the aquatic environment (environmental protection). In particular, COD and BOD_5 must be below 30 and 90 mg/L according to the Tunisian standard NT.106.002 (1989).

The current methods for pollutant removal from wastewater are still expensive and requires many resources [8].Recent attention has focused on the use of nanomaterials to reduce COD and BOD_5 levels as strategy for addressing ecosystem safety concerns. Nanotechnology based attempts have been made using magnetic nanoparticles (MNPs) for removal of organic pollutants and heavy metals from running water and wastewater [9].

The use of MNPs is highly desirable in many ways, some properties and responses can be mentioned, for instance: high specific surface interaction with molecules and ions (surface to volume ratio); high absorption efficiency [10] ; lack of penetration resistance due to the elimination of the interior absorption surfaces in porous adsorbent [11]; and the capacity of efficient removal from the water after the treatment using magnets [12]. These properties from MNPs are strongly dependent on characteristics such as composition, size, morphology, magnetic properties as well as surface area and defects.

Iron oxides received a great deal of attention on water treatment strategies account of their magnetic properties. The use of magnetite (Fe_3O_4) has been explored as remediation agents in advanced oxidation processes [13], magnetized coagulation [14] , or absorption and removal of pollutants from water as recyclable heterogeneous catalyst [15]. MNPs composed of Fe_3O_4 as a catalyst support have been studied due to its size and shape control as well as its non-toxic properties [16].

Different synthesis methods have been developed to produce Fe_3O_4 MNPs with good control over particle properties. Combustion synthesis is a simple and low-cost method to obtain MNPs that can be scaled up for environmental applications. Previously, Ianoş et all [26] demonstrated that combustion synthesis of Fe_3O_4 was influenced by the reaction atmosphere and the fuel used. Mukasyan AS and Dinka P.t [27] showed that using the combustion method MNPs with extremely high surface area could be synthesized.

Applications of MNPs exploits the basic mechanisms of magnetic coupling between an external magnetic field and the MNPs magnetic moments for the purpose of extracting impurities from water. It enhances the process of impurity removal by allowing for efficient and selective separation of the targeted contaminants from the fluid stream.[28] The process involves a coating of the adsorbent material or embedding a magnetic substance within different molecules. By the use of a magnetic field gradient, which generates a magnetic force on the MNPs, they can be effortlessly separated from the fluid stream by an appropriate design of a magnetic field. Magnetic coupling can also boost the overall efficiency of the impurity removal process. It selectively targets specific contaminants, thus improving the efficacy of the adsorption process, which leads to higher removal rates and more effective treatment of polluted water.[29]

 doi:10.20944/preprints202309.1243.v2

The effects of the application of a magnetic field on the efficiency for reduction of organic compounds in wastewater by magnetite nanoparticles has been investigated [30]. The application of the magnetic field favors the disturbance of the laminar flow, thus generating useful mixing patterns to promote the intimate interaction of the nanoparticles with other components present in the solution. This was also evidenced by better suspension of the nanoparticles as the magnetic field was increased. In (Zieliski et al., 2014)[32]study, the ideal activity of magnetite NPs was accomplished after 48 hours by appalling a magnetic field of 20.0 mT, a temperature of 20 to 40 °C, and a pH of 6 to 10.

This work shows results on the efficiency of MNPs for removal of COD and BOD_5 in polluted water from Wadi El Bey River (Tunisia). The removal efficiency was enhanced by 15 % by combining Fe_3O_4 nanoparticles with a magnetic field. The magnetic field enhances the removal of COD and BOD5 and assists in the separation of MNPs.

2. Materials and Methods

2.1. Synthesis of MNPS

The reagents used for combustion synthesis of the magnetic material were: Ferric nitrate nonahydrate ($Fe(NO_3)_3 9H_2O$, Sigma-Aldrich ≥99.95%) as raw reactant and glycine ($C_2H_5NO_2$, Sigma-Aldrich) as fuel. A schematic representation of the employed methodology is presented in Figure 1.

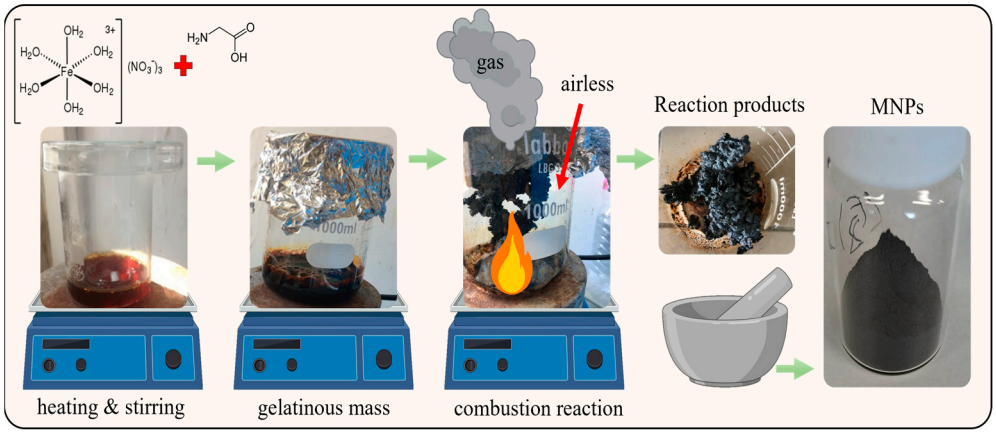

Figure 1. Steps of the performed combustion method. After mixing the raw reactant and the fuel, the combustion reaction products were grinded until reaching fine powder composed by magnetic nanoparticles (MNPs).

First, $Fe(NO_3)_3$ and $C_2H_5NO_2$ were dissolved in 150 mL of deionized water under stirring to prepare homogeneous solution. Then, the solution was poured into 1000 mL beaker and heated contentiously on a temperature controlled hot plate until evaporation and evolving into a viscous gelatinous mass. After several minutes, a violent self-propagating and non-explosive combustion reaction suddenly took place, leading to the formation of MNPs, accompanied by the liberation of voluminous gases. The result of the combustion reaction was recovered and grinded in a mortar until reach a fine powder. This powder was stored at room temperature for further characterization.

2.2. Characterization techniques

Physical and chemical properties from the obtained MNPs were characterized using different techniques. Morphology and particle size were determined using Transmission Electron Microscopy (TEM) image analysis using a FEG TECNAI T20 at 200 kV and ImageJ software. Diluted dispersions containing MNPs were prepared and a 10 µl drop were placed on Holley-carbon copper grids for the observations and images obtention. The crystal structure of the as prepared product was examined using a Bruker D8 Advance high-resolution X-ray powder diffractometer (XRD) using Cu Kα radiation (λ=1.5418 Å) in Bragg-Brentano configuration. For compositional analysis, Perkin Elmer

 doi:10.20944/preprints202309.1243.v2

Frontier Fourier Transform Infrared (FTIR) spectrometer for the identification of molecular vibrations in the samples, and energy dispersive spectroscopy (EDS) was developed using a Quanta FEG 650 Scanning Electron Microscope (SEM) equipped with Harvard® X-Ray photon detector. Surface area and porous size measurements were performed using 120 mg of as prepared MNPs in a TriStar 3000 (Micromeritics) analyzer and the calculations were obtained using the TriStar 3000 V6.08 A software.

2.3. COD and BOD5 measurements

Previously collected samples, from the river´s effluent, were filtered in order to avoid affecting test results from turbidity. Standard methods for the testing polluted water were used to measure the values of COD and BOD5 according to the protocol referenced in the Standard Water and Wastewater Testing Methods (COD and 5210-B Part 5220-B) (Baird et al., 2012) at 174 and 340mg/l, respectively.

For the COD measurements, the water samples (2 ml) were placed in a culture tube and 1 ml of $K_2Cr_2O_7$ was added to the solution. Then, the sulfuric acid reagent solution (3 mL) was carefully poured into the container to form an acid layer below the sample digest layer. The tube containing the mixture was placed in a block cooker preheated to 150°C and refluxed for 2 hours. Then, after cooling the sample to room temperature, 2 drops of ferritin indicator are added to the solution under stirring and titrated with standard 0.10M FAS. At the end, the color change from blue-green to reddish-brown.

BOD5 was measured by the respiration method, which allows the direct measurement of the oxygen consumption of microorganisms from air or an oxygen-enriched environment in a closed vessel under constant and stirred conditions. Respirometry measures oxygen consumption continuously over time. The oxygen tank is the column of air above the sample. As with standard methods, dilution is required. Vials are hermetically sealed to prevent interference from external atmospheric pressure. Oxygen is provided by constant stirring (a magnetic stir bar helps diffuse oxygen into the sample). Carbon dioxide is formed when heterotrophic bacteria oxidize organic matter.

As CO_2 is produced, it is removed from the system by absorbing sodium hydroxide and the pressure change is recorded. The change in pressure is directly proportional to the CO_2 produced. ie O_2 consumed, the final value was converted to an equivalent BOD value (Eaton et al. 1998). The amount and removal efficiency (%) of COD and BOD5 (mg/g) on MNPs at each time point were calculated by the following equation (1) (Yazdanbakhsh et al. 2015).

$$R\% = \frac{C_0 - C_f}{C_0} \quad (1)$$

Where C_0 and C_f are the initial and final concentrations of COD and BOD5 (mg/L).

The COD and BOD5 assessments were evaluated in function of different experimental parameters: contact time; concentration of MNPs, pH and stirring rate speed.

3. Results

3.1. MNPs size and structure

The bright field TEM image of the obtained MNPs presented in Figure 2a show the typical agglomerated state expected when it comes to magnetic nanostructures. Large clusters were founded during the sample's observation, but results evident that those clusters are composed by small particles. As inset in Figure 2a), the histogram from particle size distribution analysis (n= 200 particles) shown that most of the particles in the sample fall within a certain size range around the average ($\phi = 17 \pm 6$ nm), but there may also be some particles that are larger or smaller.

 doi:10.20944/preprints202309.1243.v2

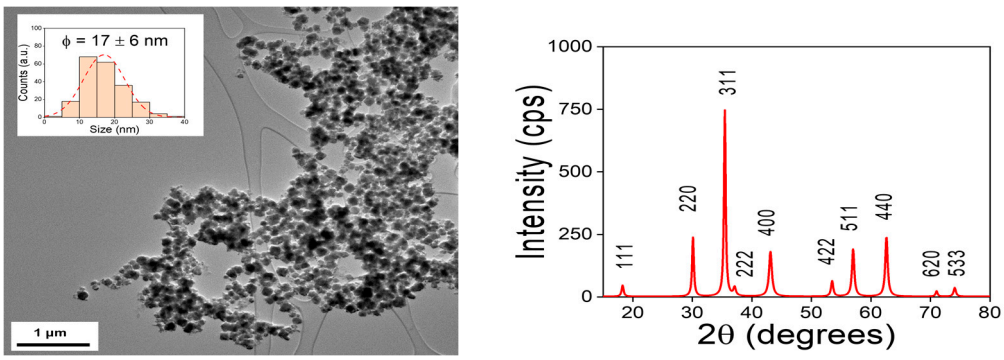

(**a**) (**b**)

Figure 2. Particle size and structure of MNPs produced by the combustion method: (**a**) bright field TEM micrograph of MNPs samples, and as inset size distribution histogram revealing average diameter ϕ= 17 ± 6 nm; (**b**) X-ray diffractogram from powder samples of as-obtained MNPs identifying the different crystalline planes reflections associated to the magnetite structure (JCPDS 19-629).

The XRD patterns from obtained MNPs presented in Figure 2 b) is associated to magnetite (Fe_3O_4) compound. All diffraction peaks of the X-ray diffractogram are indexed according to JCPDS 19-629 of magnetite-type iron oxide. The elaborated MNPs belong to the space group Fd-3m whose mesh parameter is a = 8.3940 Å.[33] The peak width and absence of unexplained peaks confirmed the crystallization and high purity of the nanoparticle-sized magnetite. The average crystal size of magnetite nanoparticles was estimated using equation (2)[34]

$$D = \frac{K*\lambda}{\beta*cos\theta} \quad (2)$$

Where D is the average crystal size, λ is the X-ray radiation's wavelength (1.5406 Å), K is the dimensionless form factor (0.9, in this case), β is the line's FWHM (full width at half maximum) in radians, and θ is the Bragg's angle in degrees [35]The FWHM of the major peak (2θ = 35.405°) of XRD patterns, the nanomaterials that were synthesized had an average crystalline size of about 17.6 nm.

3.2. MNPs composition

Examination of the FTIR spectrum shows a strong absorption band at 560 cm^{-1} assigned to stretching vibration of Fe-O functional groups typical of the crystalline lattice of magnetite (Fe_3O_4). [3637] [38] The intense band at 1380 cm^{-1} and centered at 1100 cm^{-1} are due to residual NH_4^+ in prepared simple. Vibration detected in 1040 cm^{-1} is associated to the CO-O-CO tension in carbon dioxide released during combustion. Other materials vibration modes are appeared at 3500 cm^{-1} and 1750 cm^{-1} are attributed to hydrogen-bonded water molecules vibrations adsorbed on the surface and O-H bending vibration [39] [40]. Our result is in agreement with the results of other works, which affirmed that the presence of magnetite can be seen by wide strong absorption band between 540 and 630 cm^{-1} [41], especially for Fe–O bond of bulk magnetite at 576 cm^{-1}. Referring to the work of [42] magnetite can be presented in the form of crystals with continuous bonds and the atoms are bound together with equal forces (ionic, covalent or van der vales force). According to these results, the vibration modes appeared at around 440cm^{-1} and 560cm^{-1} are related to Fe-O bonds and are respectively attributed to octahedral and tetrahedral sites.[43].

The secondary electron SEM micrograph presented in Figure 2 b) reveal the large clusters formed by the agglomeration on MNPs in powder. Some authors suggested that the agglomeration of nanoparticles was caused by the Van Der Waals forces due to operating conditions and drying.[44] Also, the presence of residual water enhances the agglomeration of nanoparticles with nanometric size in the order of several micrometers. The obtained EDS spectrum confirms the presence of elements Fe (73.24%), O (20.39 %) and C (6.37%) in the sample.

 doi:10.20944/preprints202309.1243.v2

3.3. MNPs surface area analysis

The powder specific surface area and porosity distribution of MNPs were analyzed using BET technique. These parameters are critical in determining the ability to adsorb and remove various molecules from contaminated water. The obtained BET surface area of 16.82 ± 0.01 m^2/g. While the pore volume about 0.04 cm^3/g and the pore size 10.66 nm.

According to the isotherm shown in Figure 3, the obtained MNP behaves like a type II isotherm, this type of isotherm indicates an indefinite multi-layer formation after completion of the monolayer and is found in adsorbents with a wide distribution of pore sizes (inset). When a monolayer is completed, successive layers adsorption occurs forming the observed inflexion point. This behavior is characteristic of adsorbents that they are capable to adsorb more efficiently the gas molecules, for instance water vapor on activated carbon[45]. However, the large surface area of MNPs is suitable for adsorption and heterogeneous surfaces for be reached using this kind of materials. Moreover, functional groups present on the MNPs surfaces can improve the interactions with ions, molecules and large particles present in the waste water from the Wadi El Bey watershed.

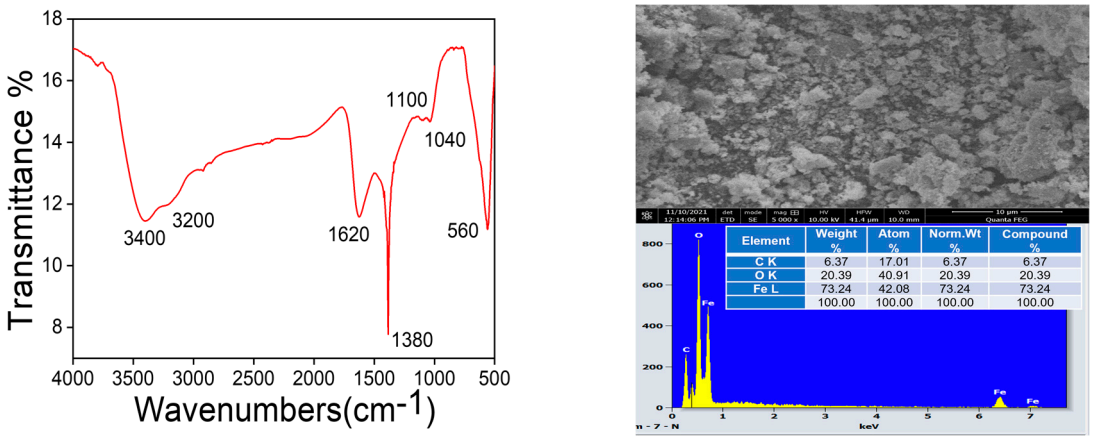

(**a**) (**b**)

Figure 3. MNPs composition: (**a**) vibrational normal modes from MNPs functional groups detected in FTIR-ATR; (**b**) secondary electrons SEM image showing agglomerated clusters and EDS spectrum at 10 kV from MNPs samples in powder.

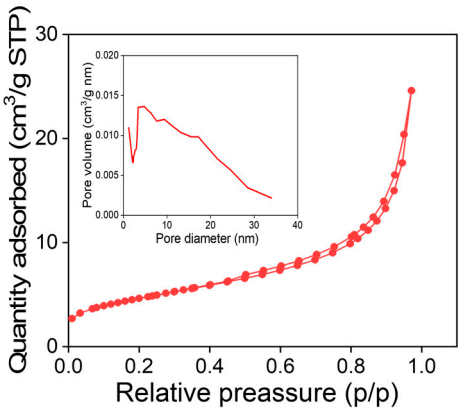

Figure 3. N_2 adsorption isotherm from MNPs elaborated using combustion method, as inset broad pore diameter distribution can be observed.

3.4. Removal efficiency using MNPs within the BOD_5 and COD experiements

The obtained MNPs were evaluated as water´s quality enhancers in a series of experiments to observe the effect of the different experimental conditions on its performance reducing BOD_5 and

 doi:10.20944/preprints202309.1243.v2

COD. The Figure 4 summarizes the results from the experiments using MNPs under different contact time (Figure 4 a)), concentration (Figure 4 b)), pH (Figure 4 c)), and stirring velocity (Figure 4 d)).

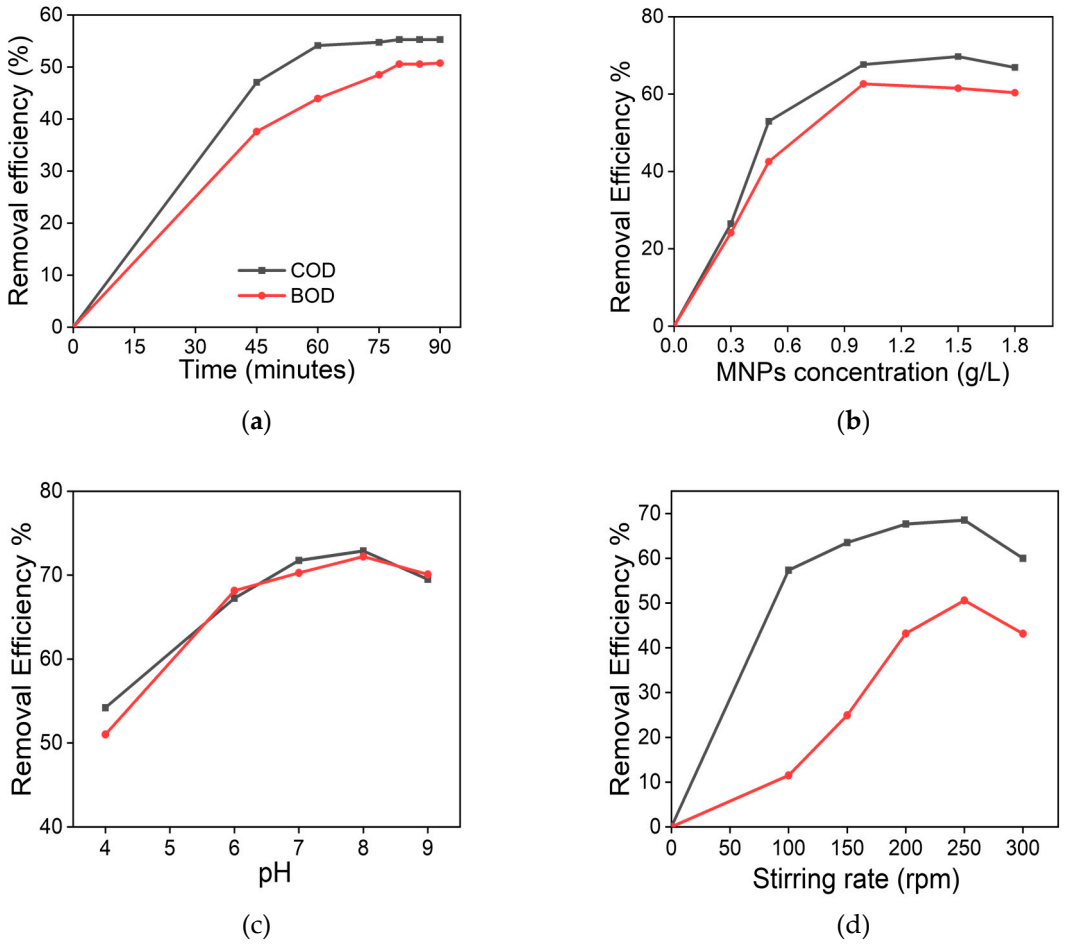

Figure 4. COD and BOD_5 removal efficiency using MNPs at different experimental conditions: (**a**) the effect of the contact time using 1 g/L of MNPs at 45-90 minutes interval; (**b**) the effect of MNPs using 0.3-1.8 g/L concentrations, pH=8; (**c**) the effect of the pH conditions, evaluating from 4 to 9 values (1 g/L of MNPs, 200 rpm); and (**d**) the stirring rate effect evaluated from 100 to 300 rpm during 80 minutes.

The optimal contact time was evaluated using 1 g/L of MNP in the experiment. The pH value of the polluted water was kept at 8, and the stirring speed was about 200 rpm at a room temperature of 20±1°C. Times of 45, 60, 75, 80, 85 and 90 minutes, respectively were evaluated during the experiments. The obtained results showed that the high values of COD and BOD_5 removal efficiencies reached 55% and 50% within 80 minutes at the lowest limit. However, the results showed that the COD and BOD_5 removal efficiencies stabilized after a contact time of 80 min.

Using 80 minutes as optimal parameter, the COD and BOD_5 were evaluated using different concentrations of MNPs, ranging 0.3-1.8 g/L. The removal efficiency was increased as the MNPs concentration increased as can be observed in Figure 4 d), but some differences were founded between COD and BOD_5. For COD, the removal efficiency reaches their maximum (70%) at 1.5 g/L MNPs doses, whereas for BOD_5, the optimal value of MNPs concentration was founded at 1 g/L for removal efficiency of 63 %.

The influence of the pH on the reduction of oxidizable components in waste water using MNPs were explored emulating acidic, neutral, and alkaline conditions (pH 4, 6, 7, 8, and 9) for COD and BOD_5 concentrations (340 and 174 mg/L, respectively), using 1 g/L of MNPs and contact period 80 min as optimal parameters with stirring rate 200 rpm at ambient temperature 25± 1 °C. The removal

 doi:10.20944/preprints202309.1243.v2

efficiency for COD and BOD_5 were 54, 67, 71, 73, 70 % and 51, 68, 70, 72, and 70 %. Therefore, a value of pH=8 was selected as the optimal condition for removal efficiency.

Stirring speed was also a factor studied for removal efficiency of COD and BOD_5, since the unavoidable agglomeration of the MNPs in aqueous solutions could influence the results. We evaluated stirring speeds ranging from 100 to 300 rpm. The removal efficiencies in function of the agitation speed for COD and BOD_5 can be observed in Figure 4 d). Removal efficiency of 57, 63, 67, 68, and 60% for COD and 12, 25, 43, 50 and 43 % for BOD_5 were obtained, choosing 250 rpm as the best agitation value.

Using the previously set of parameters as the most efficient for removal of COD and BOD_5 in polluted water, we aimed to minimize the variability in the results from MNPs coagulation y applying an external dc magnetic field of H = 0.33 T keeping the contact time of 80 min, pH of 8, MNPs concentration of 1.5 g/L, and a stirring speed of 250 rpm. The results in Figure 5 shows a clear COD removal increase from 61% to 76%, and from 63% to 77% on BOD_5 measurements.

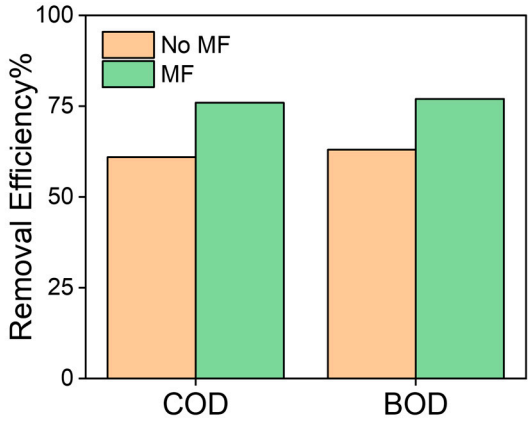

Figure 5. Improvement on removal efficiency of oxidizable pollutants in waste water using magnetic nanoparticles and magnetic separation (0.33 T).

4. Discussion

The characterization results positioning to the combustion method employed for the synthesis as feasible method to produce on a facile way MNPs with adequate properties such as size, crystallinity, surficial area and functional groups for their application as removal agents in the oxidizable pollutant removal applications.

In the evaluation of MNPs as enhancers of the quality of water, some findings can be summarized as follows. The contact time must be at least 80 minutes to achieve maximum efficiency (Figure 7). In a previous work of Ahmed S. Mahmoud et all [46], the effect of contact time on COD and BOD_5 removal efficiency using green synthesis nano-iron extracted from black tea has been studied. They found that the optimal time was 60 min with a removal efficiency of 87.9 and 100 % for COD and BOD_5 respectively. Moreover, Rasha A. Sary El-deen et all worked on the removal of COD from Domestic Wastewater using Entrapped Sewage Sludge Ash and the effective time was 60 min with a removal efficiency of 78% for an initial COD concentration 400 mg/L[47]

In the work of Rabie S. Farag et all who studied the removal of chemical oxygen demand from aqueous solution using the expensive nano zero valent iron (nZVI) compared to Fe_3O_4, the optimum removal time was 20 min for COD removal[48]. Also, Nashaat N. Nassar et all who worked on the treatment of olive mill based wastewater by means of magnetic nanoparticles the effective time for COD removal was 30 min.[49] In general, literature findings showed that the optimal time for COD and BOD_5 removal using magnetite NPs is between 20 and 120 min and our result is similar with most works.

Many researchers have proven that the increasing of adsorbent quantity will increase the number of active sites, adsorbent surface and availability of molecules to adsorbent surface. So, the probability of contact and adsorption will increase while increasing the mass of nanoparticles But, by increasing the amount of adsorbent, the risk of formation of solid aggregate and the decrease in apparent porosity and also the decrease in nanoparticle mobility will cause a difficulty in the diffusion of molecules in the adsorbent and will then decrease the efficiency of adsorption.

We can then conclude that the optimal mass of magnetite nanoparticles is 1.5 g/L. The difference in absorptionBOD_5 and COD is due to differences in the carbon chain, the solubility of ingredients them and surface tension to the absorbent surface. The similar results were reported in elimination of aniline and surfactant and total organic carbon with Fe_3O_4 nanoparticles and activated carbon-Fe_3O_4.

The results show that the removal efficiency was the highest at pH = 8 under slightly alkaline conditions. This result can be attributed to the strongly acidic medium, where small magnetite particles are decomposed under the influence of acid, leaving NPs in vacancies and affecting the adsorption activity. On the other hand, the excess OH- ions in the strong alkaline solution can enhance the removal rate of COD and BOD5 by activating the adsorption sites with negatively charged ions. In this case, similar results were obtained by many researchers [50] using different adsorbent materials for sewage removal, showing an effective pH = 8.

Stirring speed of 250 rpm seemed enough to allow maximum adsorption conditions (i.e., avoiding coagulation while adsorption onto the MNPs takes place), with no further removal effectiveness at higher stirring speeds. Previous investigations reported the removal of COD from aqueous solutions using conventional methods, such as SSA adsorption and aluminum sulfate coagulation that took place between 200 and 500 rpm, consistent with these results [51] .

Magnetite nanoparticles of Fe_3O_4 are known to act as efficient adsorbents[52], due to the hydroxyl groups on the surface of Fe_3O_4 that can generate positive or negative charges through protonation or deprotonation by pH changes in aqueous solution, making this material a good option to adsorb and remove ionic species from water through electrostatic interactions [53] .The positively-charged Fe ions in Fe_3O_4 also serve as adsorption sites for negatively charged species or electron-rich functional groups of certain organic pollutants. Furthermore, the surface of Fe_3O_4 can be modified to improve functionalization and protect the core from demagnetization [54]

The present results reveal that the adsorption performance of Fe_3O_4 can be enhanced by magnetic coupling to remove COD and BOD_5. Based on the work of Brown and Barnwell [55] a strong correlation was found between different types of microorganisms and the horizontal magnetic field vector. This study also supports Tomska and Wolny's observation of increased degradation of organic matter [56] . They showed that nitrogen compounds respond positively to an MF (magnetic field) with an induction strength of 40 mT. The good adsorption efficiency and high recoverability of the Fe_3O_4 MNPs using magnetic fields, together with the low cost and potential scalability of their production to match industrial requirements, make this approach competitive as a future strategy against the hurdles of large basin-s wastewater decontamination.

Author Contributions: Conceptualization, J.A.F.G ,H.T,A.E and M.F. ; methodology, J.A.F.G ,H.T,A.E ,M.F and G.F.G.; software, A.E and M.F; validation, H.T, A.E, M.F,K.H.N, and J.A.F.G.; formal analysis H.T; investigation KHN.; resources, H.T.; data curation, H.T ,A.E and M.F.; writing—original draft preparation, HT, J.A.F.G.; writing—review and editing, G.F.G. MF.; supervision, M.F.; funding acquisition, G.F.G. K.H.N All authors have read and agreed to the published version of the manuscript.".

Funding: This research was partially funded by Project PDC2021-121409-I00 (MICRODIAL) MCIN/AEI/10.13039/501100011033 through the European Union "NextGenerationEU"/PRTR".

Acknowledgments: JAFG and GFG acknowledged the Agencia Estatal de Investigación (AEI) for partial financial support. HT, AE and MF acknowleged The Ministry of Higher Education and Scientific Research of Tunisia for their continuous encouragement by project of young Reasearch 20JPEC04-03.

Conflicts of Interest: The authors declare no conflict of interest.

References

1. Wang, Y.; Wang, P.; Bai, Y.; Tian, Z.; Li, J.; Shao, X.; MUS-TAVICH, L. F. 6. *LI BL 7*, 30–40.
2. Ahmed, W.; Vieritz, A.; Goonetilleke, A.; Gardner, T. Health Risk from the Use of Roof-Harvested Rainwater in Southeast Queensland, Australia, as Potable or Nonpotable Water, Determined Using Quantitative Microbial Risk Assessment. *Applied and Environmental Microbiology 76* (22), 7382–7391.
3. Davies, J. M.; Mazumder, A. Health and Environmental Policy Issues in Canada: The Role of Watershed Management in Sustaining Clean Drinking Water Quality at Surface Sources. *Journal of Environmental Management* **2003**, *68* (3), 273–286. https://doi.org/10.1016/S0301-4797(03)00070-7.
4. Louati, M. E. H.; Khanfir, R.; Alouini, A.; El Echi, M. L.; Frigui, L.; Marzouk, A. Guide Pratique de Gestion de La Sécheresse En Tunisie. *Approche méthodologique. Ministére de l'Agriculture*.
5. Khadhar, S.; Mlayah, A.; Chekirben, A.; Charef, A.; Methammam, M.; Nouha, S.; Khemais, Z. Vecteur de La Pollution Metallique Du Bassin Versant de l'Oued El Bey Vers Le Golfe de Tunis (Tunisie. *Hydrological sciences journal 58* (8), 1803–1812 ,.
6. Gasmi, T.; Khouni, I.; Ghrabi, A. Assessment of Heavy Metals Pollution Using Multivariate Statistical Analysis Methods in Wadi El Bey (Tunisia). *Desalination and Water Treatment* **2016**, *57* (46), 22152–22165. https://doi.org/10.1080/19443994.2016.1147377.
7. Dębska, K.; Rutkowska, B.; Szulc, W.; Gozdowski, D. Changes in Selected Water Quality Parameters in the Utrata River as a Function of Catchment Area Land Use. *Water 13* (21), 2989.
8. Wu, H.; Zhang, J.; Ngo, H. H.; Guo, W.; Hu, Z.; Liang, S.; Liu, H. A Review on the Sustainability of Constructed Wetlands for Wastewater Treatment: Design and Operation. *Bioresource technology 175*, 594–601.
9. Shukla, S.; Khan, R.; Daverey, A. Synthesis and Characterization of Magnetic Nanoparticles, and Their Applications in Wastewater Treatment: A Review. *Environmental Technology and Innovation* **2021**, *24*, 101924. https://doi.org/10.1016/j.eti.2021.101924.
10. Fortes, C. C. S.; Daniel-da-Silva, A. L.; Xavier, A. M. R. B.; Tavares, A. P. M. Optimization of Enzyme Immobilization on Functionalized Magnetic Nanoparticles for Laccase Biocatalytic Reactions. *Chemical Engineering and Processing: Process Intensification* **2017**, *117* (March), 1–8. https://doi.org/10.1016/j.cep.2017.03.009.
11. Mohsenibandpei, A.; Ghaderpoori, M.; Hassani, G.; Bahrami, H.; Bahmani, Z.; Alinejad, A. A. Water Solution Polishing of Nitrate Using Potassium Permanganate Modified Zeolite: Parametric Experiments, Kinetics and Equilibrium Analysis. *Global Nest Journal* **2016**, *18* (3), 546–558. https://doi.org/10.30955/gnj.001833.
12. Liu, J. F.; Zhao, Z. S.; Jiang, G. Bin. Coating Fe3O4 Magnetic Nanoparticles with Humic Acid for High Efficient Removal of Heavy Metals in Water. *Environmental Science and Technology* **2008**, *42* (18), 6949–6954. https://doi.org/10.1021/es800924c.
13. Marcinowski, P.; Bury, D.; Krupa, M.; Ścieżyńska, D.; Prabhu, P.; Bogacki, J. Magnetite and Hematite in Advanced Oxidation Processes Application for Cosmetic Wastewater Treatment. *Processes* **2020**, *8* (11), 1–17. https://doi.org/10.3390/pr8111343.
14. Sibiya, N. P.; Rathilal, S.; Tetteh, E. K.; Amo-Duodu, G. Evaluation Of The Effect Of Recycled Magnetized Coagulants On Wastewater Treatment. *Journal of Pharmaceutical Negative Results* **2022**, *13*, 3466–3472. https://doi.org/10.47750/pnr.2022.13.S09.431.
15. Lourens, A.; Falch, A.; Malgas-Enus, R. Magnetite Immobilized Metal Nanoparticles in the Treatment and Removal of Pollutants from Wastewater: A Review. *Journal of Materials Science* **2023**, *58* (7), 2951–2970. https://doi.org/10.1007/s10853-023-08167-2.
16. Masudi, A.; Harimisa, G. E.; Ghafar, N. A.; Jusoh, N. W. C. Magnetite-Based Catalysts for Wastewater Treatment. *Environmental Science and Pollution Research* **2020**, *27* (5), 4664–4682. https://doi.org/10.1007/s11356-019-07415-w.
17. Jeong, J. R.; Shin, S. C.; Lee, S. J.; Kim, J. D. Magnetic Properties of Superparamagnetic γ-Fe2O3 Nanoparticles Prepared by Coprecipitation Technique. *Journal of magnetism and magnetic materials 286*, 5–9.
18. Khomane, R. B.; Agrawal, A.; Kulkarni, B. D. Synthesis and Characterization of Lithium Aluminate Nanoparticles. *Materials Letters 61* (23–24), 4540–4544.
19. Dumitrache, F.; Morjan, I.; Alexandrescu, R.; Ciupina, V.; Prodan, G.; Voicu, I.; Soare, I. Iron–Iron Oxide Core–Shell Nanoparticles Synthesized by Laser Pyrolysis Followed by Superficial Oxidation. *Applied Surface Science 247* (1–4), 25–31.

20. Cheng, P.; Li, W.; Liu, H.; Gu, M.; Shangguah, W. Influence of Zinc Ferrite Doping on the Optical Properties and Phase Transformation of Titania Powders Prepared by Sol–Gel Method. *Materials Science and Engineering: A 386* (1–2), 43–47.
21. Cannas, C.; Concas, G.; Gatteschi, D.; Musinu, A. N. N. A.; Piccaluga, G.; Sangregorio, C. How to Tailor Maghemite Particle Size in γ-Fe 2 O 3–SiO 2 Nanocomposites. *Journal of Materials Chemistry 12* (10), 3141–3146.
22. Kwon, S. W.; Park, S. B. Effect of Precursors on the Morphology of Lithium Aluminate Prepared by Hydrothermal Treatment. *Journal of materials science 35*, 1973–1978.
23. Asuha, S.; Suyala, B.; Siqintana, X.; Zhao, S. Direct Synthesis of Fe3O4 Nanopowder by Thermal Decomposition of Fe–Urea Complex and Its Properties. *Journal of Alloys and Compounds 509* (6), 2870–2873.
24. Moore, J. J.; Feng, H. J. Combustion Synthesis of Advanced Materials: Part I. Reaction Parameters. *Progress in materials science 39* (4–5), 243–273.
25. Ekambaram, S.; Patil, K. C.; Maaza, M. Synthesis of Lamp Phosphors: Facile Combustion Approach. *Journal of Alloys and Compounds 393* (1–2), 81–92.
26. Ianoş, R.; Lazău, I.; Păcurariu, C. The Influence of Combustion Synthesis Conditions on the α-Al 2 O 3 Powder Preparation. *Journal of materials science 44*, 1016–1023.
27. Mukasyan, A. S.; Dinka, P. Novel Approaches to Solution-Combustion Synthesis of Nanomaterials. *International Journal of Self-Propagating High-Temperature Synthesis 16*, 23–35.
28. Elaoud, A.; Turki, N.; Amor, H. Ben; Jalel, R.; Salah, N. Ben. Influence of the Magnetic Device on Water Quality and Production of Melon. **2016**, No. December. https://doi.org/10.14741/Ijcet/22774106/6.6.2016.48.
29. Amor, H. Ben; Elaoud, A. Characteristic Study of Some Parameters of Soil Irrigated by Magnetized Waters. **2020**.
30. Shukla, S.; Khan, R.; Daverey, A. Synthesis and Characterization of Magnetic Nanoparticles, and Their Applications in Wastewater Treatment: A Review. *Environmental Technology & Innovation 24*, 101924.
31. Peñaranda, P. A.; Noguera, M. J.; Florez, S. L.; Husserl, J.; Ornelas-Soto, N.; Cruz, J. C.; Osma, J. F. Treatment of Wastewater, Phenols and Dyes Using Novel Magnetic Torus Microreactors and Laccase Immobilized on Magnetite Nanoparticles. *Nanomaterials 12* (10), 1688.
32. Zieliński, M.; Dębowski, M.; Krzemieniewski, M. Effect of Constant Magnetic Field (CMF) with Various Values of Magnetic Induction on Effectiveness of Dairy Wastewater Treatment under Anaerobic Conditions. *Polish Journal of Environmental*.
33. Karimi, E.; Jeffryes, C.; Yazdian, F.; Akhavan Sepahi, A.; Hatamian, A.; Rasekh, B.; Ashrafi, S. J. DBT Desulfurization by Decorating Rhodococcus Erythropolis IGTS8 Using Magnetic Fe3O4 Nanoparticles in a Bioreactor. *Engineering in Life Sciences 17* (5), 528–535.
34. Yan, H.; Zhang, J.; You, C.; Song, Z.; Yu, B.; Shen, Y. Influences of Different Synthesis Conditions on Properties of Fe3O4 Nanoparticles. *Materials Chemistry and Physics 113* (1), 46–52.
35. Ali, A.; Chiang, Y. W.; Santos, R. M. X-Ray Diffraction Techniques for Mineral Characterization: A Review for Engineers of the Fundamentals, Applications, and Research Directions. *Minerals 12* (2), 205.
36. Flood-Garibay, J. A.; Méndez-Rojas, M. A. Synthesis and Characterization of Magnetic Wrinkled Mesoporous Silica Nanocomposites Containing Fe3O4 or CoFe2O4 Nanoparticles for Potential Biomedical Applications. *Colloids and Surfaces A: Physicochemical and Engineering Aspects 615*, 126236.
37. Li, G. Y.; Jiang, Y. R.; Huang, K. L.; Ding, P.; Chen, J. Preparation and Properties of Magnetic Fe3O4–Chitosan Nanoparticles. *Journal of alloys and compounds 466* (1–2), 451–456.
38. Nigam, S.; Barick, K. C.; Bahadur, D. Development of Citrate-Stabilized Fe3O4 Nanoparticles: Conjugation and Release of Doxorubicin for Therapeutic Applications. *Journal of Magnetism and Magnetic Materials 323* (2), 237–243.
39. Frost, R. L.; Weier, M. L.; Kloprogge, J. T. Raman Spectroscopy of Some Natural Hydrotalcites with Sulphate and Carbonate in the Interlayer. *Journal of Raman Spectroscopy 34* (10), 760–768.
40. Innocenzi, P.; Falcaro, P.; Grosso, D.; Babonneau, F. Order− Disorder Transitions and Evolution of Silica Structure in Self-Assembled Mesostructured Silica Films Studied through FTIR Spectroscopy. *The Journal of Physical Chemistry B 107* (20), 4711–4717 8.
41. Ma, M.; Zhang, Y.; Yu, W.; Shen, H. Y.; Zhang, H. Q.; Gu, N. Preparation and Characterization of Magnetite Nanoparticles Coated by Amino Silane. *Colloids and Surfaces A: physicochemical and engineering aspects 212* (2–3), 219–226.
42. Waldron, R. D. Infrared Spectra of Ferrites. *Physical review 99* (6), 1727.

43. Gasparov, L. V; Tanner, D. B.; Romero, D. B.; Berger, H.; Margaritondo, G.; Forro, L. Infrared and Raman Studies of the Verwey Transition in Magnetite. *Physical Review B 62* (12), 7939.
44. Maharaj, D.; Bhushan, B. Effect of Spherical Au Nanoparticles on Nanofriction and Wear Reduction in Dry and Liquid Environments. *Beilstein journal of nanotechnology 3* (1), 759–772.
45. Saleh, T. A. Isotherm Models of Adsorption Processes on Adsorbents and Nanoadsorbents. *Interface Science and Technology* **2022**, *34*, 99–126. https://doi.org/10.1016/B978-0-12-849876-7.00009-9.
46. Mahmoud, A. S.; Farag, R. S.; Elshfai, M. M. Reduction of Organic Matter from Municipal Wastewater at Low Cost Using Green Synthesis Nano Iron Extracted from Black Tea: Artificial Intelligence with Regression Analysis. *Egyptian Journal of Petroleum 29* (1), 9–20.
47. Saryel-Deen, R. A.; Mahmoud, A. S.; Mahmoud, M.; Mostafa, M. K.; Peters, R. W. Adsorption and Kinetic Studies of Using Entrapped Sewage Sludge Ash in the Removal of Chemical Oxygen Demand from Domestic Wastewater, with Artificial Intelligence Approach. In *2017 Annual AIChE Meeting*.
48. Farag, R. S.; Elshfai, M. M.; Mahmoud, A. S.; Mostafa, M. K.; Karam, A.; Peters, R. W. (670d) Study the Degradation and Adsorption Processes of Organic Matters from Domestic Wastewater Using Chemically Prepared and Green Synthesized Nano Zero-Valent Iron. *AIChE Annual Meeting, Conference Proceedings* **2019**, *2019-Novem* (November).
49. Nassar, N. N.; Arar, L. A.; Marei, N. N.; Ghanim, M. M. A.; Dwekat, M. S.; Sawalha, S. H. Treatment of Olive Mill Based Wastewater by Means of Magnetic Nanoparticles: Decolourization, Dephenolization and COD Removal. *Environmental Nanotechnology, Monitoring & Management 1*, 14–23.
50. Sahu, O. P.; Chaudhari, P. K. Review on Chemical Treatment of Industrial Waste Water. *Journal of Applied Sciences and Environmental Management 17* (2), 241–257.
51. Mahmoud, A. S.; Farag, R. S.; Elshfai, M. M. Reduction of Organic Matter from Municipal Wastewater at Low Cost Using Green Synthesis Nano Iron Extracted from Black Tea: Artificial Intelligence with Regression Analysis. *Egyptian Journal of Petroleum 29* (1), 9–20.
52. Cao, M.; Li, Z.; Wang, J.; Ge, W.; Yue, T.; Li, R.; William, W. Y. Food Related Applications of Magnetic Iron Oxide Nanoparticles: Enzyme Immobilization, Protein Purification, and Food Analysis. *Trends in Food Science & Technology 27* (1), 47–56.
53. Phouthavong, V.; Yan, R.; Nijpanich, S.; Hagio, T.; Ichino, R.; Kong, L.; Li, L. Magnetic Adsorbents for Wastewater Treatment: Advancements in Their Synthesis Methods. *Materials 15* (3), 1053.
54. Cao, M.; Li, Z.; Wang, J.; Ge, W.; Yue, T.; Li, R.; William, W. Y. Food Related Applications of Magnetic Iron Oxide Nanoparticles: Enzyme Immobilization, Protein Purification, and Food Analysis. *Trends in Food Science & Technology 27* (1), 47–56.
55. Barnwell, F. H.; Brown, F. A. Responses of Planarians and Snails. In *Biological Effects of Magnetic Fields*; Barnothy, M. F., Ed.; Springer US: Boston, MA, 1964; pp 263–278. https://doi.org/10.1007/978-1-4899-6578-3_25.
56. Tomska, A.; Wolny, L. Enhancement of Biological Wastewater Treatment by Magnetic Field Exposure. *Desalination* **2008**, *222* (1–3), 368–373. https://doi.org/10.1016/j.desal.2007.01.144.